6-1-2014

Simultaneous Measurement of Temperature and Pressure with Cascaded Extrinsic Fabry-Perot Interferometer and Intrinsic Fabry-Perot Interferometer Sensors

Yinan Zhang

Jie Huang
Missouri University of Science and Technology, jieh@mst.edu

Xinwei Lan

Lei Yuan

et. al. For a complete list of authors, see http://scholarsmine.mst.edu/ele_comeng_facwork/3263

Recommended Citation

Simultaneous measurement of temperature and pressure with cascaded extrinsic Fabry–Perot interferometer and intrinsic Fabry–Perot interferometer sensors

Yinan Zhang,[a] Jie Huang,[b] Xinwei Lan,[b] Lei Yuan,[b] and Hai Xiao[b,*]
[a]Missouri University of Science and Technology, Department of Electrical and Computer Engineering, 1870 Miner Circle, Rolla, Missouri 65409-0140
[b]Clemson University, Department of Electrical and Computer Engineering, Clemson, South Carolina 29634-0915

Abstract. This paper presents an approach for simultaneous measurement of temperature and pressure using miniaturized fiber inline sensors. The approach utilizes the cascaded optical fiber inline intrinsic Fabry–Perot interferometer and extrinsic Fabry–Perot interferometer as temperature and pressure sensing elements, respectively. A CO_2 laser was used to create a loss between them to balance their reflection power levels. The multiplexed signals were demodulated using a Fast Fourier transform-based wavelength tracking method. Experimental results showed that the sensing system could measure temperature and pressure unambiguously in a pressure range of 0 to 6.895×10^5 Pa and a temperature range from 20°C to 700°C. © *The Authors. Published by SPIE under a Creative Commons Attribution 3.0 Unported License. Distribution or reproduction of this work in whole or in part requires full attribution of the original publication, including its DOI.* [DOI: [10.1117/1.OE.53.6.067101](10.1117/1.OE.53.6.067101)]

1 Introduction

Pressure and temperature are two important parameters in the well and reservoir down-hole monitoring. Accurate, continuous, and real-time data of pressure and temperature helps in oil and reservoir management.[1] Sensors with dual-parameter sensing capability and survivability in the down-hole harsh environment are highly necessary in such applications. Fiber-optic sensors, with advantages such as small size, low loss, high sensitivity, resistance to harsh environments, and multiplexing capability, are good candidates for pressure and temperature down-hole monitoring.

In the past years, several types of fiber optic sensors have been demonstrated for pressure and temperature sensing. The major types include fiber Bragg grating (FBG) for temperature or dual parameters' measurement,[2–5] diaphragm-based Fabry–Perot interferometer (FPI) for pressure sensing,[6,7] long-period fiber grating for temperature sensing,[8] etc. An early reported type used a single FBG that was half encapsulated and the other half fixed in a polymer-filled metal cylinder.[2] Because the resonance wavelength shift of the FBG is affected by both temperature and pressure, the cross sensitivity becomes an issue. Double FBG coated by a special polymer in a metal tube was later developed to discriminate between pressure and temperature.[3] FBGs in specialty fibers have also been proposed, e.g., FBGs in standard and grapefruit microstructure fibers.[9] However, the ultraviolet laser-induced FBG has a maximum temperature limit of around 200°C. Recently, a combined pressure–temperature sensor consisting of two low-finesse Fabry–Perot resonators was reported.[10] This structure provides a potential for high-temperature applications. However, the fabrication process involves hydrogen fluoride (HF) etching which is hazardous.

This article presents a new method for dual-parameter sensing using the cascaded intrinsic Fabry–Perot interferometer (IFPI) and extrinsic Fabry–Perot interferometer (EFPI) sensors. These sensors are fabricated using a femtosecond (fs) laser. The IFPI is constituted of a pair of fs laser-induced internal reflectors. The EFPI is positioned at the fiber tip and consists of an fs laser thinned silica diaphragm and a sealed air cavity.

2 Sensor Fabrication and Principle

2.1 Sensor Fabrication

The proposed sensor consists of a pair of cascaded IFPI and EFPI, as shown in Fig. 1(a). The IFPI is formed by two internal partial reflectors created by an fs laser in the core of a single-mode fiber (SMF). It is sensitive to temperature due to the combination of the thermo-optic effect and thermal expansion of the fiber material. However, the IFPI is insensitive to pressure. The EFPI is located at the fiber tip, formed by the fiber endface and a thin silica diaphragm which deflects under pressure, providing the pressure sensing function.

Sensor fabrication consists of the following steps. First, the EFPI was fabricated at the tip of a single-mode fiber. A section of hollow core silica capillary tube with an outer diameter of 150 μm and an inner diameter of 75 μm (TSP075150, Polymicro Inc., Pheonix, Arizona) was initially spliced to a standard single-mode fiber (Corning SMF-28e). Then the tube was cleaved at a distance (tens of micrometers) from the splice point with the help of a microscope. The tube was then spliced to another SMF to form a sealed air cavity sandwiched between two fibers. Precision fiber cleaving was applied to cut the fiber so that a thin piece of fiber was left to perform as a diaphragm. Finally, the as-cleaved diaphragm was thinned and roughened by an fs laser (Coherent RegA 9000, 200-fs pulse

*Address all correspondence to: Hai Xiao, E-mail: haix@clemson.edu
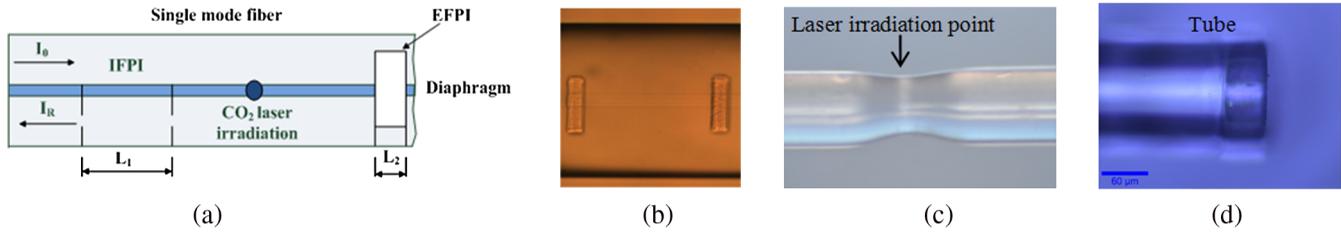
Fig. 1 (a) Scheme of the proposed sensor, (b) photo of IFPI, (c) photo of CO_2 laser irradiation point and (d) photo of EFPI.

duration, 250-kHz repetition rate, and 800-nm wavelength). The fs laser micromachining method was described in detail in our previous publication.[11] The fs laser fabrication method has several advantages, including precise control of the diaphragm thickness, immunity to the refractive index variations of the surrounding medium, and ease of signal processing. Figure 1(d) shows the image of an EFPI fabricated using this method.

Next, an IFPI was fabricated at a short distance (~1 cm) away from the EFPI. It was created by inscribing two parallel lines in the fiber core with the fs laser. A water immersion lens (Olympus UMPlanFL 20×) was used to focus the fs laser beam into the fiber core. Figure 1(b) shows the microscopic image of an IFPI. The two parallel lines in the fiber core are clearly observed.

With the above fabrication procedure, an IFPI with a cavity length L_1 of a few hundred micrometers and an EFPI with a cavity length L_2 of tens of micrometers were successfully produced. L_1 was set to be significantly longer than L_2 to facilitate signal processing, which will be discussed later.

The refractive index change in the fiber core induced by the fs laser is very small (10^{-4} to 10^{-2}); therefore, the reflectivity of the internal reflectors in an IFPI is far lower than the reflectivity of an air/glass interface in an EFPI (4%). Due to the unbalanced reflectivity, there is a difference of 20 to 30 dB in their intensity levels. The intensity level of the IFPI signal is so low that it can hardly be observed in the spectrum.

One method to balance the power levels of the IFPI and EFPI signals is to add a transmission loss between the IFPI and EFPI. In this paper, a CO_2 laser (SYNRAD, Inc., Mukilteo, Washington) with a free-space wavelength of 10.6 μm was employed to heat the fiber to increase the transmission loss. A ZnSe cylindrical lens with a focal length of 50 mm was used to shape the CO_2 laser beam into a narrow line with a linewidth of about 220 μm. The CO_2 laser was controlled by a computer so that the output power and exposure duration could be accurately adjusted. During fabrication, the CO_2 laser heated the fiber and created a microbend between EFPI and IFPI, as shown in Fig. 1(c). An optical spectrum analyzer (Ando AQ 6319) was used to monitor the reflection spectrum. The power and duration time of the CO_2 laser were set to 12 W and 200 ms, and the irradiation process was repeated multiple times until an ideal spectrum was obtained.

2.2 Sensor Principle

The temperature sensitivity of a Fabry–Perot sensor is contributed by the thermo-optic and thermal-expansion effects,

$$K_T = (\alpha_{TO} + \alpha_{CTE})\lambda_v, \tag{1}$$

where α_{TO} is the thermo-optic coefficient, α_{CTE} is the coefficient of thermal expansion, and λ_v is the wavelength of an interference valley. The typical values of the fused silica are 8.3×10^{-6}°C^{-1} and 5.5×10^{-7}°C^{-1}, respectively,[12] so an IFPI thermo-optic effect plays a major role in its temperature sensitivity. However, in an air-cavity based EFPI, the thermo-expansion effect plays a dominant role.

In an EFPI, the diaphragm deflection–induced cavity length change under pressure is[13]

$$S = \frac{3(1 - \mu^2)a^4}{16Eh^3} \ (\mu\text{m/Pa}), \tag{2}$$

where a and h are the diaphragm radius and thickness (in μm), respectively. E and μ are Young's modulus and Poisson's ratio of the diaphragm material.

The wavelength shift of an interference valley as a function of pressure is

$$\Delta\lambda = \lambda_v \frac{S}{L} \Delta P, \tag{3}$$

where L is the EFPI cavity length and ΔP is the pressure change.

Therefore, the pressure sensitivity coefficient $K_{P,EFPI}$ as a function of the wavelength shift can be obtained from Eqs. (2) and (3).

2.3 Signal Processing

When temperature and pressure are simultaneously applied, the wavelength shifts of the IFPI and EFPI can be expressed as

$$\Delta\lambda_{IFPI} = K_{P,IFPI} \times \Delta P + K_{T,IFPI} \times \Delta T \tag{4}$$

and

$$\Delta\lambda_{EFPI} = K_{P,EFPI} \times \Delta P + K_{T,EFPI} \times \Delta T. \tag{5}$$

The temperature and pressure can be obtained by solving the following characteristic matrix

$$\begin{bmatrix} \Delta T \\ \Delta P \end{bmatrix} = \frac{1}{\Omega} \begin{pmatrix} K_{P,EFPI} & -K_{P,IFPI} \\ -K_{T,EFPI} & K_{T,IFPI} \end{pmatrix} \begin{bmatrix} \Delta_{\lambda,IFPI} \\ \Delta_{\lambda,EFPI} \end{bmatrix}, \tag{6}$$

where $\Omega = K_{P,EFPI}K_{T,IFPI} - K_{T,EFPI}K_{P,IFPI}$.

The interference signals of the EFPI and IFPI sensors are multiplexed. The fast Fourier transform (FFT) is a widely
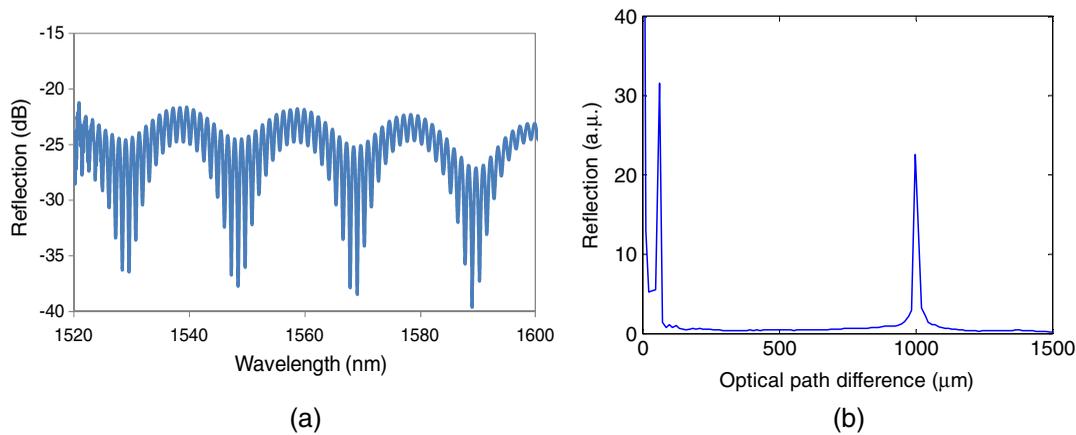
Fig. 2 (a) Spectrum of multiplexed EFPI and IFPI sensors and (b) FFT of the multiplexed sensor spectrum.

used method to demodulate multiplexed FPI signals. By performing the Fourier transform on the recorded interferogram, the optical path difference (OPD) of each FPI can be resolved. The minimum detectable OPD change is given by[14]

$$\Delta l = \frac{\pi}{\nu_E - \nu_S}, \tag{7}$$

where ν_E and ν_S are the smallest and largest wavenumbers in the measurement range, respectively.

According to Eq. (7), for a broadband light source with a wavelength range from 1520 to 1620 nm, Δl is approximately 12 μm. Due to the low resolution, FFT is not suitable for signal demodulation when the cavity length change is small. Recently, a FFT-based wavelength tracking method to demodulate multiplexed IFPI signals was proposed.[15] This method uses band-pass filters to extract specific frequency components and transform them back to the wavelength domain and then uses the wavelength tracking method to find the OPD change. As a result, the measurement accuracy has been significantly improved.

Figure 2(a) plots the recorded spectrum of the multiplexed IFPI and EFPI sensors, and Fig. 2(b) plots the FFT of the spectrum. Two main frequency components with substantially different OPDs can be clearly identified, corresponding to the EFPI and IFPI, respectively. The OPD for IFPI is the

refractive index of the fiber core ($n = 1.4682$) times the physical cavity length, so the cavity lengths of the EFPI and IFPI are calculated to be 62 and 680 μm, respectively.

Two Hamming-windowed digital filters were used to select each frequency component. After filtering, an interference spectrum was reconstructed using an inverse FFT. Figures 3(a) and 3(b) plot the reconstructed waveforms of the EFPI and IFPI, respectively.

Once the individual interferograms of the EFPI and IFPI are obtained, we can pick a specific interference valley in the reconstructed waveform as the tracking wavelength. Then the wavelength tracking method was used to obtain the wavelength shifts of the interferograms.

3 Experimental Results

The experimental setup for sensor characterization is illustrated in Fig. 4. The light from a 100-nm bandwidth ASE light source (BWC-ASE) was launched into the sensor via a 3-dB fiber coupler. The sensor was sealed in a Swagelok tube where the air pressure was supplied using a compressed Argon gas cylinder and controlled by a pressure controller (MKS640). The pressure controller/generator could provide a static pressure up to 6.895×10^5 Pa with a precision of ∼0.5%. The Swagelok tube-sealed sensor was then placed in a programmable electrical furnace
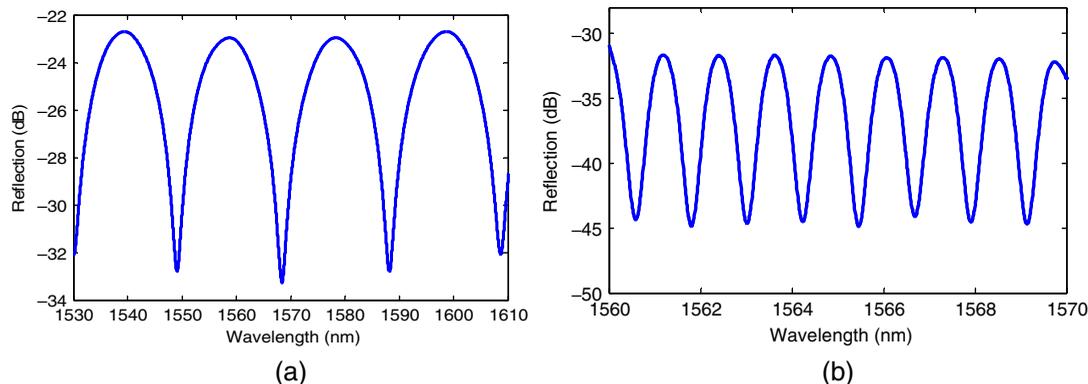
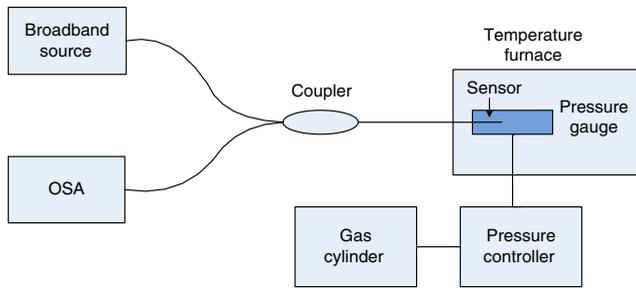**Fig. 3** Reconstructed waveforms of (a) EFPI and (b) IFPI.

Fig. 4 Experiment setup for sensor test.

Table 1 Calibration results.

Coefficient	$K_{T,EFPI}$ (nm/°C)	$K_{P,EFPI}$ (nm/Pa)	$K_{T,IFPI}$ (nm/°C)	$K_{P,IFPI}$
Value	0.001	1×10^{-6}	0.0146	0

(Lindberg/blue M) whose temperature could be varied from room temperature to 1100°C. The sensor output signal was recorded using an optical spectrum analyzer.

First, the temperature and pressure sensitivities for the EFPI and IFPI sensors were calibrated. The calibration results are listed in Table 1. As we expected, the IFPI is primarily temperature sensitive but pressure insensitive. On the other hand, the EFPI is primarily pressure sensitive but temperature insensitive.

Next, the sensor was tested for simultaneous pressure and temperature measurements. The measurement procedure was described as follows. Given a constant temperature, the pressure was increased from 0 to 6.895×10^5 Pa at an increment of 1.379×10^5 Pa. Under a constant pressure, the temperature was set to increase from room temperature (20°C) to 700°C at increments of 50°C.

Figure 5(a) shows the measured pressure results of the hybrid sensor at the temperatures of 20°C, 400°C, and 700°C. Figure 5(b) shows the measured temperature results of the hybrid sensor at different pressures of 0, 3.447×10^5, and 6.895×10^5 Pa. The temperature and pressure data were

taken directly from the electrical furnace and the pressure controller readings, respectively. Linear approximation curves were added to show the linearity of the measurement results. As shown in Fig. 5, the hybrid sensor successfully decoupled the temperature and pressure. The maximal measured discrepancy among individually measured pressures at three temperatures was 4×10^3 Pa, in the pressure range of 0 to 6.895×10^5 Pa. The maximal measured discrepancy among individually measured temperatures at three pressures was 0.8°C, in the temperature range of 20°C to 700°C. The discrepancies were within the range of instrument uncertainties and the resolution limit of the used optical spectrum analyzer.

4 Conclusion

In this article, we reported a miniature, all-fiber IFPI and EFPI hybrid sensor suitable for simultaneous measurement of temperature and pressure. The IFPI was fabricated using an fs laser to micromachine two reflectors inside the core of a single-mode fiber. The IFPI was primarily sensitive to temperature but insensitive to pressure variations. The EFPI was fabricated by fusion-splicing a fused silica capillary tube between two single-mode fibers and precision-cleaving of a fiber to form a thin diaphragm-sealed cavity. The diaphragm was further thinned by fs laser ablation which allowed for precise control of the diaphragm thickness and immunity to the refractive index variations of the surrounding medium. Because of the diaphragm sealed air-cavity structure, the EFPI is primarily sensitive to pressure but insensitive to temperature. A CO_2 laser was used for the creation of an attenuator to balance the reflected power levels of the two sensors for easy signal processing and sensor demultiplexing. The EFPI and IFPI were designed to have significantly different OPDs and the multiplexed interference signals were demodulated using an FFT-based wavelength tracking method. The hybrid sensor was tested for simultaneous measurements of pressure and temperature in a temperature range from 20°C to 700°C and a pressure range from 0 to 6.895×10^5 Pa. The results showed complete decoupling between the pressure and temperature. The good linearity in the measurement range and the simultaneous measurement capability of the demonstrated sensor provide the potential for down-hole monitoring in high temperature and pressure harsh environments.
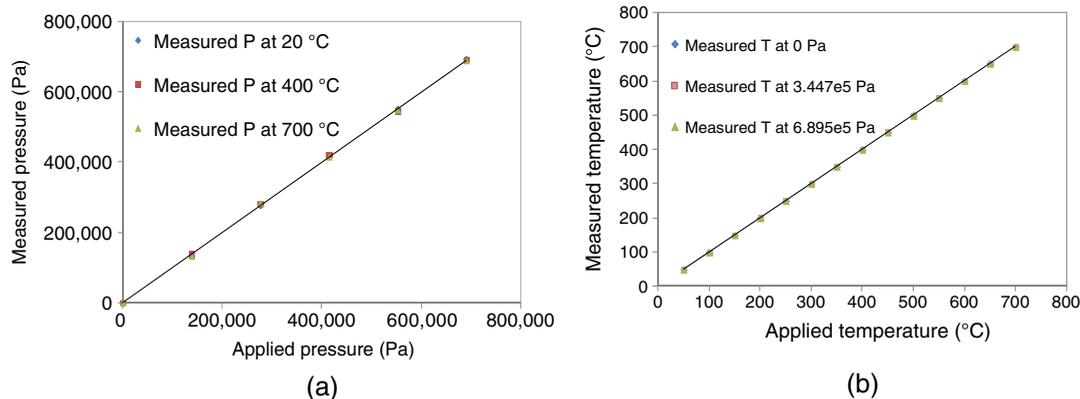

(a)

(b)

Fig. 5 (a) Pressure measurement results under different temperatures and (b) temperature measurement results under different pressures.

References

1. G. Fusiek, P. Niewczas, and J. R. McDonald, "Design of a highly accurate optical sensor system for pressure and temperature monitoring in oil wells," in *IEEE I2MTC 2009*, Singapore, pp. 574–578 (2009).
2. A. Sun et al., "Study of simultaneous measurement of temperature and pressure using double fiber Bragg gratings with polymer package," *Opt. Eng.* **44**(3), 034402 (2005).
3. Y. Liu et al., "Simultaneous pressure and temperature measurement with polymer-coated fiber Bragg grating," *Electron. Lett.* **36**, 564–566 (2000).
4. E. Chmielewska, W. Urbanczyk, and W. Bock, "Measurement of pressure and temperature sensitivities of a Bragg grating imprinted in a highly birefringent side-hole fiber," *Appl. Opt.* **42**, 6284–6291 (2003).
5. T. Guo et al., "Simultaneous measurement of temperature and pressure by a single fiber Bragg grating with a broadened reflection spectrum," *Appl. Opt.* **45**, 2935–2939 (2006).
6. K. Bremer et al., "Conception and preliminary evaluation of an optical fibre sensor for simultaneous measurement of pressure and temperature," in *Journal of Physics: Conf. Series*, Edinburgh, UK (2006).
7. S. H. Aref et al., "Fiber optic Fabry–Perot pressure sensor with low sensitivity to temperature changes for downhole application," *Opt. Commun.* **269**, 322–330, (2007).
8. Y. L. Wang et al., "Simultaneous temperature and pressure measurement using a packaged FBG and LPG," in *15th IEEE OECC 2010*, Sapporo, pp. 814–815, IEEE (2010).
9. C. Wu, Y. Zhang, and B. Guan, "Simultaneous measurement of temperature and hydrostatic pressure using Bragg gratings in standard and grapefruit microstructured fibers," *IEEE Sens. J.* **11**, 489–492 (2011).
10. S. Pevec and D. Donlagic, "Miniature all-fiber Fabry-Perot sensor for simultaneous measurement of pressure and temperature," *Appl. Opt.* **51**, 4536–4541 (2012).
11. Y. Zhang et al., "High-temperature fiber-optic Fabry Perot interferometric pressure sensor fabricated by femtosecond laser," *Opt. Lett.* **38**, 4609–4612 (2013).
12. S. Takahashi and S. Shibata, "Thermal variation of attenuation for optical fibers," *J. Non-Cryst. Solids* **30**, 359–370 (1979).
13. M. D. Giovanni, *Flat and Corrugated Diaphragm Design Handbook*, 1st ed., Marcel Dekker Inc., New York (1982).
14. Y. Huang et al., "An extrinsic Fabry–Perot interferometer-based large strain sensor with high resolution," *Meas. Sci. Technol.* **21**, 105308 (2010).
15. W. Wang et al., "Quasi-distributed IFPI sensing system demultiplexed with FFT-based wavelength tracking method," *IEEE Sens. J.* **12**, 2875–2880 (2012).

Yinan Zhang received her MS and PhD degree in electrical engineering from Missouri University of Science and Technology in 2010 and 2013, respectively. Her research interests include optical fiber sensors, optical coherence tomography, etc. She is a member of IEEE, SPIE, and OSA.

Jie Huang received his BS degree in optoelectronic engineering from Tianjin University, Tianjin, China, in 2009 and MS degree in electrical engineering from Missouri University of Science and Technology, Rolla, in 2012. He is currently pursuing his PhD degree in electrical engineering at Clemson University. His research interest mainly focuses on the development of photonics and microwave sensors and instrumentations for applications in energy, intelligent infrastructure, and biomedical sensing.

Xinwei Lan received his PhD degree in electrical engineering from Missouri University of Science and Technology, 2013. He is currently a research associate at the Center for Optical Materials Science and Engineering Technologies (COMSET), Clemson University. His research efforts have been dedicated to developing novel optical and microwave sensors for harsh environment sensing, chemical/biological sensing and structure health monitoring. He is a member of the OSA, IEEE, ACS, and SPIE.

Lei Yuan received his BS degree in mechanical engineering from Beijing University of Aeronautics and Astronautics, Beijing, China, in 2008. He is currently pursuing his PhD degree in electrical engineering at Clemson University, Clemson, USA. His research interests mainly focus on laser micro/nano fabrication as well as fiber optic sensors and devices for various engineering applications. He is a student member of OSA and SPIE.

Hai Xiao is the Samuel Lewis Bell Distinguished Professor at Clemson University. He was previously a professor of electrical engineering at the Missouri University of Science and Technology. He received his PhD degree in electrical engineering from Virginia Tech in 2000. His research interests focus on photonic and microwave sensors and instrumentation for applications in energy, intelligent infrastructure, clean environment, national security, biomedical sensing and imaging.